Contents lists available at ScienceDirect

Transportation Research Part C

journal homepage: www.elsevier.com

# The feasibility of Follow-the-Greens for 4-dimensional trajectory based airport ground movements

Tianci Zhang [a], Michal Weiszer [b], Jun Chen [b,*]

[a] College of Automobile and Traffic Engineering, Nanjing Forestry University, 159 Longpan Road, Nanjing 210037, China
[b] School of Engineering and Materials Science, Queen Mary University of London, Mile End Road, London E1 4NS, UK

ARTICLE INFO

*Keywords:*
Airport ground movements
4-Dimensional trajectory (4DT)
Follow-the-Greens (FtG)
Guidance
Control theoretic model

ABSTRACT

Safer and more efficient airport ground movements can be planned by routing and scheduling systems based on the 4-dimensional trajectory (4DT). In order to achieve the benefits envisioned in the planning stage, an effective taxiing guidance system is indispensable. The Follow-the-Greens (FtG) guidance concept provides an augmented means for 4DT based taxiing with pilot in the loop, which is expected to guide the piloted aircraft by dynamically adjusting the lit position of green ground navigation lamps according to the assigned 4DTs. This paper presents a simulation study to investigate the feasibility of FtG based on a control theoretic modeling of the taxiing system. The 4DT conformance errors with different navigation lamp control strategies are investigated. The key performance indices, including temporal constraint violation and fuel consumption, are analysed. The results demonstrate that it is feasible to follow conflict-free 4DTs through FtG if an appropriate lamp controller is available. The results also highlight the need to proactively handle the potential conformance errors in the routing and scheduling stage.

## 1. Introduction

In current airport surface operations, the green navigation lamps installed on the central or side lines of the taxiway are utilised to guide the aircraft moving along the assigned taxiing route. Such ground-based taxiing guidance is referred to as Follow-the-Greens (FtG) (European Commission, 2017; Straube et al., 2017). FtG is originally included as part of the general Surface Movement Guidance and Control System (SMGCS) of an airport (Martin et al., 1998). A first implementation of the FtG system is made at London Heathrow Airport. The green lamps on the taxiway centerlines are switched on/off up to the red stopbar of the taxiway segment. The assigned taxiing route is thus indicated by the line of lit green lamps between the aircraft and the next red stopbar. Similar ground-based guidance systems are also deployed in other airports worldwide. However, the lamps are mostly switched on/off subject to manual control and no optimisation of the taxiing flow is sought.

The Advanced Surface Movement Guidance and Control System (A-SMGCS) provides a first development to optimise the taxiing phase (ICAO, 2004). To this end, a systematic expansion of automated support for taxiing participants is required. In the final stage of expansion of the A-SMGCS system, automation in route planning and support in taxiing guidance based on ground signals are planned (Eurocontrol, 2010). In this context, the use of ground lamps in A-SMGCS has been researched in several projects (Carotenuto, 2005; Katz, 2000; Urvoy, Oehme, Drege, Sendobry, & Klingauf, 2010). In the American project of Advanced Taxiway Guidance System (Katz, 2000), the suitability of automatically controlled ground lamps for the specific requirements of A-SMGCS

* Corresponding author.
*E-mail addresses:* zhangtiancy@163.com (T. Zhang); m.weiszer@qmul.ac.uk (M. Weiszer); jun.chen@qmul.ac.uk (J. Chen)

https://doi.org/10.1016/j.trc.2020.102632
Received 12 August 2019; Received in revised form 30 January 2020; Accepted 25 March 2020
Available online xxx
0968-090/

is investigated. The aim is to achieve an automatically controlled spatial guidance for taxiing aircraft. The European project of Demonstration Facilities for Airport Movement Management System demonstrates the technical feasibility of A-SMGCS (Carotenuto, 2005). In this project, the taxiing guidance is realised using ground lamps. The lamps are switched segment by segment between two stopbars, which can provide support for the pilots without changing the current practice of the taxiing process. Similarly, the German project of Competitive Airport examines the applicability of dynamically switched ground lamps for the spatial management of aircraft (Urvoy et al., 2010). In addition, it also introduces the technology of the Airfield Ground Lighting Automation System (AGLAS), which enables the control of individual ground lamps (ADB SAFEGATE, 2020). A comprehensive review of the corresponding research work can be found in Urvoy (2014).

In spite of the abovementioned research effort, it should be noted that conventional FtG can only provide spatial information of the assigned taxiing route, without temporal information such as the required arrival time at the intermediate waypoints along the route. Therefore, aircraft still have a large degree of freedom during taxiing. However, this makes it difficult to accurately predict the actual arrival time at intermediate positions of the taxiing route as well as the actual taxiing time of the aircraft (Ravizza et al., 2014a), which may not only prevent effective optimisation of taxiing speeds, but also have further implications on other airside operations (e.g. increased difficulty in runway sequencing and gate assignment). Moreover, due to the uncertainty in taxiing times, large separation has to be kept between aircraft for safety, leading to an insufficient use of airport capacity, and frequent 'stops and goes' will occur during taxiing, causing more fuel consumption and emissions (Hooey et al., 2014; Nikoleris et al., 2011).

With the advancement in information sharing among airport stakeholders (Eurocontrol, 2017) and the development of A-SMGCS technologies, the concept of trajectory-based taxiing operations (TBTO) has recently been proposed (Okuniek et al., 2016). TBTO aims to realise more precise control of airport ground movements via the assigned 4-dimensional trajectories (4DTs). In addition to the taxiing route, a 4DT also contains the information of the required arrival times at intermediate waypoints, and even the detailed speed profiles for taxiing along the route when the full 4DT is used (Weiszer et al., 2015b). The introduction of these temporal requirements makes it possible to reduce the uncertainty during taxiing (Brownlee et al., 2018) and achieve more efficient surface operations (Weiszer et al., 2015a).

In order to realise 4DT based operations in practice, a suitable guidance function needs to be in place. In addition to retrofitting the existing aircraft display systems to indicate the commanded speeds or timing information, an improved FtG function can serve as an augmented means for the purpose of 4DT based guidance. The improved FtG function will allow dynamic control of airport navigation lamps in a more granular unit, e.g. through controlling the number of lit lamps. Increasing the number of the lit lamps will indicate acceleration for the guided aircraft, and vice versa (Okuniek et al., 2016). This makes it possible to deliver both spatial and temporal information of a 4DT to the pilot. The seminal study of this guidance means can be found in Haus et al. (2011), where the authors proposed an improved FtG guidance approach based on the automatic control theory. In this approach, a first-order control theoretic model of the FtG system was developed. Different ground navigation lamp control strategies, including feed forward (FF) and proportional-integral-integral ($PI_2$) control, were exploited to automatically decide the number of lit lamps. Following this seminal study, a complete operational concept for a 4-dimensional taxiing guidance system based on FtG was developed and evaluated by airline pilots using a full flight simulator in Urvoy (2014). It showed that the predetermined 4DTs were consistently adhered to by the pilots. Satisfactory results on the situational awareness and stress of the pilots were also obtained, and the suitability for use of the developed FtG system was demonstrated.

In spite of the advancement in the guidance means, aircraft may inevitably deviate from the assigned trajectories in real-world scenarios, especially when moving under the manual control. The actual performance of 4DT based operations will thus depend on the conformance of aircraft to the assigned trajectories. Apart from potential increase in fuel consumption and emissions, small deviation from the assigned trajectory may not be detrimental. However, as the deviation grows bigger, insufficient separations between aircraft may occur, which may ultimately endanger the safety of surface operations. In TBTO, the deviation from the assigned trajectory could be more dangerous as the distance between the leading and the following aircraft on a taxiway is allowed to be smaller than in conventional surface operations due to more precise control of the taxiing trajectory. Therefore, in order to ensure effective routing and scheduling for TBTO, a comprehensive investigation of the conformance performance to the assigned 4DTs under various guidance means is pressing.

This paper presents one such investigation using FtG as the guidance means. It extends the seminal work in Haus et al. (2011) by investigating the performance of FtG in conjunction with the recently proposed 4DT planning framework (Chen et al., 2016a; Chen et al., 2016b). Based on the aircraft taxiing dynamics and pilot driving parameters identified in Haus et al. (2011), this paper focuses on evaluating the feasibility of FtG for taxiing guidance when conflict-free 4DTs are assigned to the aircraft, and probing the impact of the conformance errors with respect to the assigned 4DTs on the safety and efficiency of the ground movements. The results are expected to provide useful guidelines towards an integrated design of routing, scheduling and guidance for more robust planning and execution of the 4DTs. The main contributions of this paper are as follows:

1) The feasibility of FtG as an augmented means to provide 4-dimensional information for trajectory-based taxiing operations is studied. The study is conducted based on the control theoretic model of the FtG taxiing system, which shows that aircraft are able to follow the conflict-free 4DTs generated in the 4DT planning stage in spite of some inevitable conformance errors.
2) A proportional-integral-derivative (PID) ground navigation lamp controller is devised to improve 4DT tracking performance of aircraft, which shows superior capability to reduce the conformance error compared with the existing lamp controllers in Haus et al. (2011). This result emphasises the important role of ground navigation lamp controllers for effective FtG, and provides foundation for designing more powerful ground navigation lamp controllers to further reduce the 4DT conformance error.

3) The determination of suitable minimal time separation in the planning stage for consecutive aircraft traversing the same taxiway zone is investigated in order to absorb 4DT conformance error during taxiing. This provides useful insight in setting appropriate bounds for the conformance error, which can be used as a guideline to design the required lamp controllers. The interplay between 4DT planning and guidance demonstrated in this investigation also highlights the need to integrate routing, scheduling and guidance as the future line of research.

The rest of the paper is organised as follows: Section 2 describes the concept of FtG guidance. Section 3 presents the control theoretic modeling of the FtG system and describes its main components, including the model of aircraft taxiing dynamics, the pilot driving model and the ground navigation lamp controller. Section 4 describes the data and set-up for the simulation study and investigates the conformance error as well as its adverse impact, including the violation of the temporal constraints and the increase of the fuel consumption. Section 5 concludes the paper and presents future research directions.

## 2. The FtG guidance concept

Fig. 1 presents an illustration of the FtG guidance concept. In Fig. 1(a), the green ground navigation lamps are lit by the lamp control system, guiding the pilot to drive along the assigned taxiway. In the current FtG guidance strategy, the lamp control system usually takes all the green lamps within a taxiway segment as a control unit, which means it will turn on/off all the green lamps within a single control unit simultaneously. This lamp control strategy can hardly provide any temporal information such as the required arrival time or speed contained in the 4DTs (Tang et al., 2012). To improve the guidance capability of FtG and realise 4DT based taxiing operations, the navigation lamps should be controlled in a smaller unit or even individually as proposed in Haus et al. (2011). The lamp controller will calculate the lit position (i.e. the number of green lamps) in front of the aircraft dynamically according to the actual position and speed of the aircraft as well as the expected position and speed according to the assigned 4DT, as shown in Fig. 1(b) (Haus et al., 2011). The pilot will adjust the speed of the aircraft according to the lit position and speed of the green lamps so as to conform to the expected position and speed defined by the assigned 4DT.

It is worth noting that the FtG process is similar to car following from the pilot's perspective. The lit green lamps correspond to the leading car, while the aircraft corresponds to the following car. The pilot tries to catch up the lit green lamps by accelerating/decelerating the aircraft, which resembles the driver in the following car trying to keep pace with the leading car. As mentioned in Haus et al. (2011), it is human's intuition to follow guidance signals and, hence, FtG is an 'intuitive guidance' approach. Compared to introducing auto-brake and auto-taxiing modes in aircraft to track the 4DT as proposed in SESAR and NextGen (Schuster and Ochieng, 2014), pilots are kept in the loop in FtG, and there is no need to retrofit the onboard flight deck system.

## 3. Control theoretic modeling of taxiing with FtG guidance

In this section, a control theoretic modeling of the taxiing system with FtG guidance is presented based on the first order aircraft ground movement and pilot driving models. The structure of the system is shown in Fig. 2. $x_d$ and $x_a$ are the expected position of the aircraft defined by the assigned 4DT and the actual position of the aircraft, respectively; $x_l$ is the lit position of the green navigation lamps. An illustration of these three variables can be found in Fig. 1(b). The taxiing system consists of three modules: the model of aircraft taxiing dynamics, the pilot driving model and the lamp controller. A baseline car following model is adopted to describe the pilot driving behavior in FtG. On this basis, a PID controller is designed to calculate the lit position of the green navigation lamps, with the aim to reduce the difference between $x_a$ and $x_d$.

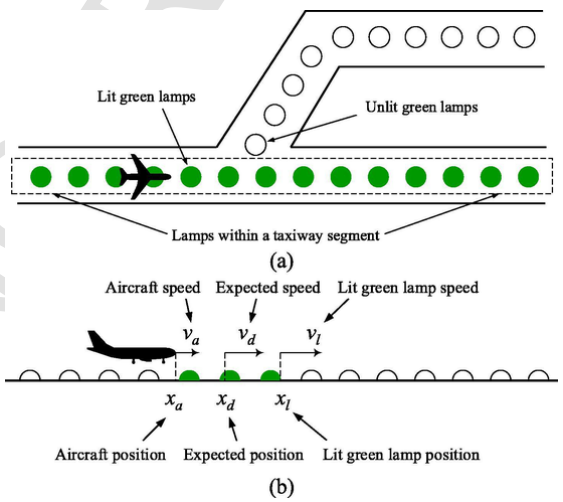


**Fig. 1.** Illustration of the FtG guidance concept. (a) The current strategy of FtG guidance. (b) FtG guidance with 4DTs.

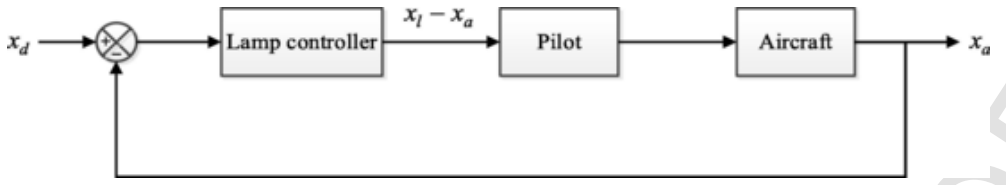


**Fig. 2.** The structure of the taxiing system with FtG guidance.

### *3.1. Aircraft taxiing dynamics*

When the lateral acceleration is ignored, the aircraft taxiing dynamics can be described by the following first order differential equation:

$$\dot{v}_a = \left(F_T - \mu m_a g - c_d v_a\right)/m_a \tag{1}$$

where $v_a$ is the aircraft taxiing speed, $m_a$ is the aircraft mass, $F_T$ is the thrust force provided by aircraft engines, $\mu$ is the rolling resistance coefficient between the aircraft tire and the ground, $g$ is the acceleration of gravity, and $c_d$ is the drag coefficient. For simplicity, $m_a$ can be approximated as a constant during taxiing. According to Eq. (1), the acceleration $\dot{v}_a$ is determined by the thrust force $F_T$ and taxiing speed $v_a$. When $F_T$ is fixed, a faster taxiing speed will result in a greater air drag and smaller acceleration rate. As the rolling resistance does not depend on the taxiing speed, Eq. (1) can be simplified by denoting the composite of $F_T$ and $\mu m_a g$ as $F$, and is described by the block diagram in Fig. 3 (Haus et al., 2011), where $K_{a,1} = 1/m_a$, $K_{a,2} = c_d$, and $1/s$ represents an integral unit (Åström and Hägglund, 2006). The system input $F$ is the output of the pilot driving model (see Section 3.2). The system output is the aircraft taxiing speed $v_a$. The integral of $v_a$ represents the actual aircraft position, which will be fed back to the navigation lamp controller (see Section 3.4).

### *3.2. Pilot driving model*

The pilot in the context of FtG resembles the driving behavior in car following. In the latter case, the main factors affecting the decision making of the driver in the following car are the relative speed and distance between the following car and the leading car. Similarly, the main factors affecting the driving behavior of the pilot are the relative speed and distance between aircraft and the lit lamp position. During taxiing, the pilot will maintain a comfortable distance to the farthest position of the lit lamps. When this distance gets too large or too small, the pilot will accelerate or decelerate accordingly to bring the distance back to the comfortable level. It is worth noting that this is a nontrivial task due to the gap between the navigation lamps installed along the taxiway as well as the pilot's reaction sensitivity to the changing distance. Consequently, there will often be delay in the pilot's actions to accelerate or decelerate, which should be considered for an effective FtG guidance design.

In light of the above discussions, the pilot driving model can be described by the block diagram shown in Fig. 4 (Haus et al., 2011). The input $x_l - x_a$ is the distance between the farthest lit lamp position $x_l$ and the actual aircraft position $x_a$. $s$ and $e^{-s\tau}$ represent a derivative and time delay unit, respectively. The relative speed $v_l - v_a$ between the aircraft and the lit lamp is obtained by differentiating $x_l - x_a$. The output of the model is the resultant force $F$, which is the input of the model of aircraft taxiing dynamics described in Section 3.1.

Parameters $K_{p,1}$ and $K_{p,2}$ account for the characteristics of pilot driving behaviors and $\tau$ represents the response time of the pilot. In order to simulate different response times of the pilots in FtG, a Monte Carlo approach is applied in the simulation study presented in this paper based on the average response time over 11 experienced pilots identified in Haus et al. (2011). Note that parameters of the pilot driving model were identified through an experiment in a fixed base flight simulator, where pilots were directed to 'Follow-the-Greens' without giving further information. A trajectory exciting the piloted aircraft system model in a sufficient frequency range was displayed to the pilots using taxiway lamps. Based on the identified model, various control strategies can be designed to automatically switch on/off the ground lamps in order to guide the pilot following the assigned 4DT. In the next sec-

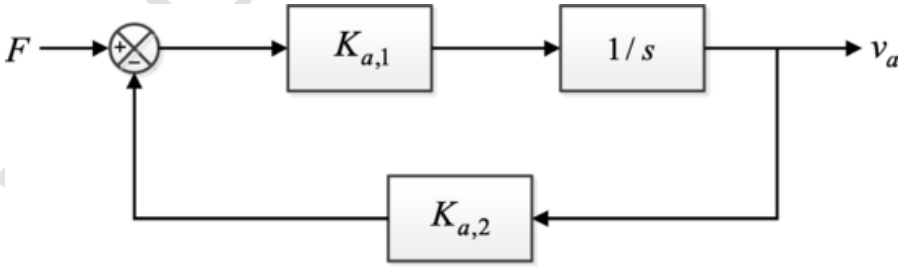


**Fig. 3.** The block diagram of aircraft taxiing dynamics.

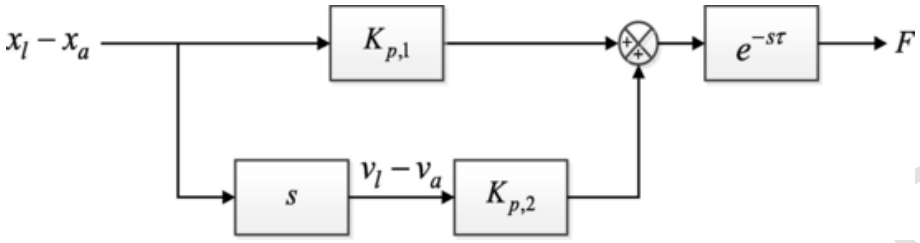


**Fig. 4.** The block diagram of the pilot driving model.

tion, an alternative lamp controller will be devised based on the same piloted aircraft system model identified in Haus et al. (2011) to improve 4DT conformance.

### *3.3. Ground navigation lamp controller*

The navigation lamp controller is critical to successful FtG guidance. For each aircraft, it dynamically adjusts the lit lamp position according to the actual aircraft position and the expected position defined by the assigned 4DT. In this paper, a PID controller is devised for this purpose which provides the control input to the pilot driving model and the model of aircraft taxiing dynamics. The block diagram of the PID controller is presented in Fig. 5. The input of the controller is the difference between the expected aircraft position $x_d$ and the actual aircraft position $x_a$. The output of the controller is the difference between the farthest lit lamp position $x_l$ and the actual aircraft position $x_a$.

When the actual aircraft position conforms to the expected position, the farthest lit lamp position will move forward according to the assigned 4DT; the pilot only needs to keep the current taxiing speed. In contrast, when the aircraft falls behind or outstrips the expected position, the lit lamp position will move faster or slower, indicating the pilot to accelerate or decelerate the aircraft.

### *3.4. The taxiing system model*

The complete taxiing system model is obtained by integrating the model of aircraft dynamics, the pilot driving model and the navigation lamp controller, as shown in Fig. 6. To avoid visually losing the guidance signals for the pilot, a limit of 0–200 m is set on the output of the lamp controller as suggested in Haus et al. (2011). However, this saturation nonlinearity would cause the phenomenon of integrator windup, leading to degradation of performance or even closed-loop instability (Hodel and Hall, 2001

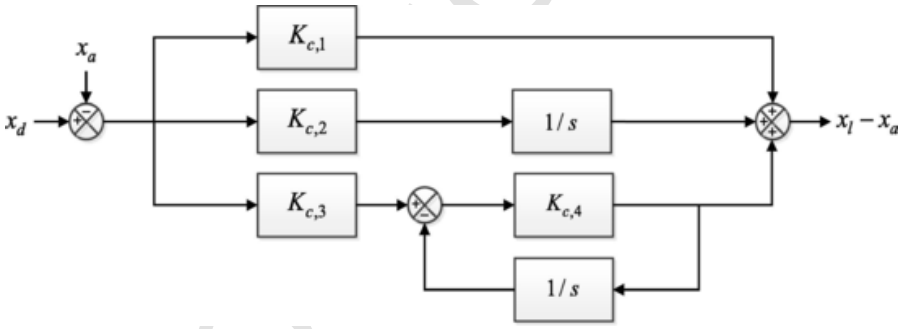


**Fig. 5.** The block diagram of the ground navigation lamp controller.

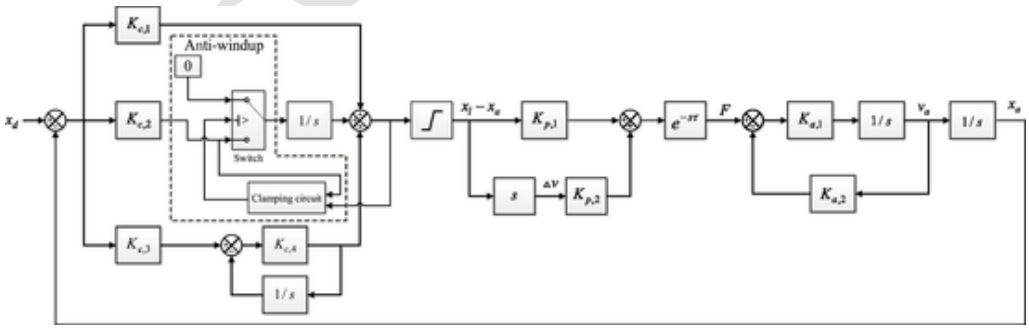


**Fig. 6.** The block diagram of the taxiing system model.

). Therefore, an anti-windup compensator is added as shown in Fig. 6 so that integration is switched off when the controller is saturated and the integrator update leads to more saturation.

## 4. Simulation results

### *4.1. Data and simulation set-up*

To investigate the performance of FtG guidance, a testing dataset for Pudong airport is generated, which includes 1234 conflict-free 4DTs, corresponding to a typical day's traffic volume of Pudong airport in 2014. These are the most fuel-efficient 4DTs under specific time constraints generated using the existing methods (Weiszer et al., 2015b; Zhang et al., 2018a, 2018b). Note that for generating the 4DTs, artificial waypoints are set along the taxiways for safe separation between aircraft during routing and scheduling, which are referred to as control points (Zhang et al., 2018b). Furthermore, taxiways are divided by the control points into smaller virtual taxiway zones (Zhang et al., 2018a). An illustration of the control points and taxiway zones is presented in Fig. 7, where the control points are represented by red circles, and zones are marked with dashed lines and labeled with texts. Each zone corresponds to a group of conflicting edges of the taxiway (denoted by solid lines between two adjacent control points), meaning it can be occupied by only one aircraft at a time, therefore ensuring safe separation distance between aircraft. In this paper, this safe separation distance is set to 50 m. The time when the zone is not occupied is denoted as a time window.

The flowchart of conflict-free 4DT generation is presented in Fig. 8. For each aircraft, a conflict-free time-based taxiing trajectory is first found using the shortest path search algorithm presented in Zhang et al. (2018a). The time-based taxiing trajectory refers to the taxiing route with required time of arrival at every zone of the taxiway along the route. If all the required times of arrival are within the calculated time windows of taxiway zones, the corresponding trajectory is conflict-free. The detailed speed profile complying with the time-based taxiing trajectory is then generated using the method presented in earlier work (Weiszer et al., 2015; Zhang et al., 2018b), providing the full 4DT for the simulation study. Here a piecewise linear speed profile model is adopted, which is applied to each edge as described in Zhang et al. (2018b). The speed profile model consists of three phases. The first and last phases correspond to a constant acceleration or deceleration rate. The second phase corresponds to a constant speed. Not all the three phases are necessarily required for each edge, as will be determined by the solution algorithm. The time windows are updated according to the newly generated 4DT to ensure conflict-free 4DT generation for the next aircraft. Additionally, a minimal time separation (similar to the buffer time described in Ravizza et al. (2014b)) $\epsilon$ is imposed between two consecutive occupancies of the same zone of the taxiway by different aircraft, which provides a tolerance for the control point arrival time deviations in a bid to absorb the 4DT conformance errors. A default minimal time separation $\epsilon = 5$ seconds will be adopted in the simulation study unless otherwise mentioned, which can effectively absorb the conformance errors for the majority of situations as shown in Section 4.3.

Typical examples of the generated 4DTs are presented in Fig. 9. In the left column of Fig. 9, the taxiing routes of the 4DTs are highlighted. In the right column, the speed profiles along the designated taxiing routes are presented. Note that dots in the speed profiles correspond to the control points (Zhang et al., 2018b).

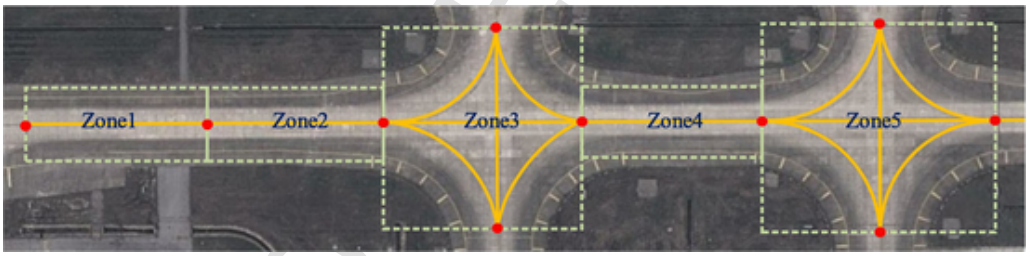


**Fig. 7.** An illustration of the control points and taxiway zones. The background satellite image of the airport is provided by Google Maps.

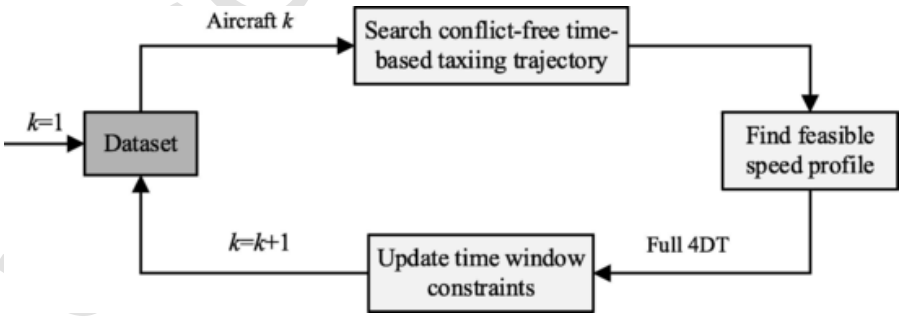


**Fig. 8.** Conflict-free 4DT generation flowchart.

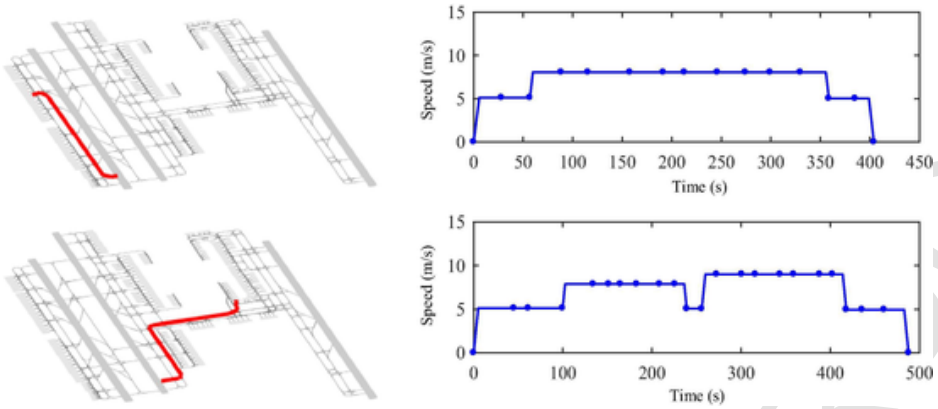


**Fig. 9.** Examples of the generated 4DTs.

After the 4DTs are generated, aircraft are simulated to follow the lamps using the taxiing system model described in Section 3.4. Without loss of generality, the model of aircraft taxiing dynamics is implemented using the parameters of Airbus A300, as shown in Table 1 (EASA, 2018; Haus et al., 2011). The fuel flow rates are used to estimate the fuel consumption in Section 4.4.

To model different pilot's reaction to the lit lamp position changes, the response time $\tau$ is a stochastic value subject to the logarithm normal distribution (Ahmed, 1999). The probability density function of $\tau$ is described in (2). $\mu$ and $\sigma$ are respectively the location and scale parameters for the normally distributed logarithm function $\ln(\tau)$. In the simulation study, we have $\mu = 1.67$ and $\sigma = 0.2$ according to the mean pilot response time $\bar{\tau} = 5.29$ seconds (Haus et al., 2011). Moreover, an upper bound of 10 s is imposed to avoid unrealistically large response time.

$$p(\tau) = \frac{1}{\tau\sigma\sqrt{2\pi}} e^{-\frac{(\ln\tau-\mu)^2}{2\sigma^2}} \tag{2}$$

The parameters of the navigation lamp controller are $K_{c,1} = 0.75$, $K_{c,2} = 0.02$, $K_{c,3} = 1.25$, and $K_{c,4} = 10$, which are determined by minimising the total conformance error for all the aircraft using particle swarm optimisation (Zhou et al., 2011). Additionally, two lamp control strategies proposed in Haus et al. (2011) are included in the study as the baselines for comparison with the PID controller. The block diagrams of the baseline lamp control strategies are presented in Fig. 10(a) and Fig. 10(b), respectively. The feed forward (FF) control in Fig. 10(a) directly switches on/off the navigation lamps according to the assigned 4DT, while a $PI_2$ controller with Smith predictor is utilised in Fig. 10(b) to control the lit lamp positions.

It should be noted that there will be inevitable 4DT conformance errors in real world scenarios due to internal and external uncertainties of aircraft (e.g. engine performance and change of the taxiway surfaces) no matter what lamp control strategies are used. Small conformance errors can lead to increase of the fuel consumption during taxiing. Large errors may lead to temporal constraint violations (i.e. more than one aircraft occupies the same zone of the taxiway simultaneously); in the worst case, the constraint violations could lead to separation loss between aircraft, impairing airport ground movement safety, or changing the orders of aircraft visiting the same taxiway. The latter case may lead to head-on encounters of aircraft and result in traffic deadlocks. For the study presented in this paper, the focus is put on investigating the feasibility of FtG as the guidance means when conflict-free 4DTs are assigned to aircraft. The potential conflicts or deadlocks caused by the 4DT conformance error are not directly handled during the simulation, as it requires the development of a sophisticated conflict detection and resolution function for 4DT based taxiing operations, which is out of the scope of this paper. In this case, the simulation for the entire testing dataset is simplified using the sequential approach described in Section 4.1 without changing the plans for the subsequent aircraft should a conflict or deadlock occur. The 4DT conformance error, the resulting constraint violations and the impact on fuel consumption are analysed according to the recorded results after running over the entire dataset.

**Table 1**
Airbus A300 parameters.

| Parameter | Value |
|---|---|
| Aircraft mass | 110000 kg |
| Rolling resistance coefficient | 0.015 |
| Drag coefficient | 466 N·s/m |
| Rated thrust | 258 kN |
| Fuel flow rate at 7% rated thrust | 0.211 kg/s |
| Fuel flow rate at 30% rated thrust | 0.682 kg/s |

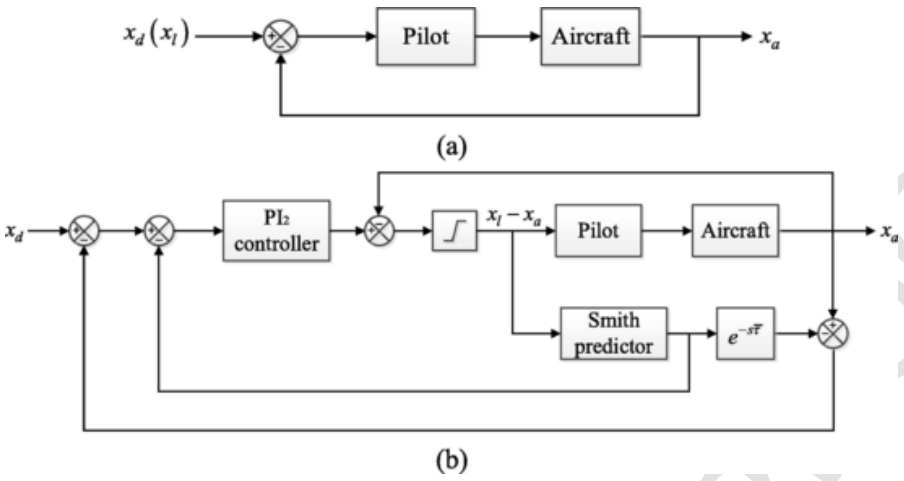


**Fig. 10.** Two alternative lamp control strategies for FtG. (a) Feed forward lamp control. (b) $PI_2$ lamp controller with Smith predictor.

Note that the conformance error in the simulation is mainly caused by the incapability of the piloted aircraft system to precisely follow the movement of lit lamps. This can be observed in the case of FF, where the movement of lit lamps simply follows the speed profile of the assigned 4DT. However, as the pilot's sensitivity to lit lamp distance changes is limited, the actual movement speed of the aircraft often deviates from the expected speed, resulting in conformance error to the assigned 4DT. Additionally, the conformance to the assigned 4DT may also be impacted by the adopted lamp controller. In the case of $PI_2$ and PID, the lamp controller can provide some decision support for the pilot (Urvoy, 2014). For example, if the aircraft falls behind the expected position due to pilot responding delay, the lit lamp position can be automatically set to a farther distance in order to timely inform the pilot about the requirement of an acceleration. Ideally, the lit lamp position should be dynamically and continuously adjusted so that any deviation from the assigned 4DT can be rapidly eliminated. However, appropriate adjustment of the lit lamp position is difficult due to the complexity of the piloted aircraft system and the variance of the expected speed. As a result, the conformance error usually still exists after using a specifically devised lamp controller. Meanwhile, it is usually possible to reduce the conformance error with more sophisticated lamp controllers.

### *4.2. 4DT conformance error*

This section analyses the 4DT conformance error using FtG as the guidance means. For clarity, the conformance error is denoted by $\triangle x_{a,d}$ ($\triangle x_{a,d} = x_a - x_d$), which is the difference between the actual aircraft position $x_a$ and the expected position $x_d$ along the taxiway central line at every time instant. When the aircraft falls behind or goes ahead of the expected position, the conformance error is a negative or positive value. In both cases, the conformance error can have adverse impact on the airport ground movements. The conformance error distributions as the results of applying the proposed PID controller and the two baseline lamp control strategies (i.e. FF and $PI_2$) are presented in Fig. 11. It can be noticed that the resulting conformance errors are similar in the cases of FF and $PI_2$, where aircraft often fall behind the expected position. When the PID controller is used, the aircraft can follow the assigned 4DT more accurately; most conformance errors are aggregated in a small range near zero.

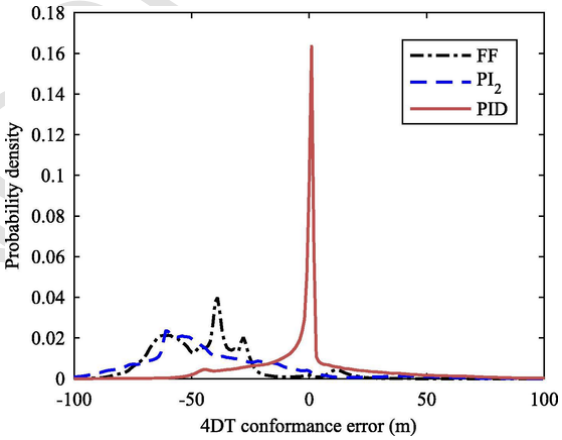


**Fig. 11.** Distributions of 4DT conformance errors using different lamp control strategies.

The mean conformance errors for different lamp control strategies are presented in Table 2. For clarity, Table 2 also presents two additional metrics of the results. The first one is the difference between the lit lamp position $x_l$ and the actual aircraft position $x_a$, which is denoted as $\triangle x_{l,a}$ ($\triangle x_{l,a} = x_l - x_a$). When the $PI_2$ or PID lamp control strategy is used, $\triangle x_{l,a}$ is always nonnegative due to the saturation limit. While in the case of FF, it is possible for aircraft to go ahead of the lit lamp position (i.e. $\triangle x_{l,a}<0$). The mean values of $\triangle x_{l,a}$ in all the three cases are similar, which correspond to the comfortable distance between the lit lamp position and the actual aircraft position that pilots usually keep during taxiing. The second metric is the difference between the lit lamp position $x_l$ and the expected aircraft position $x_d$, which is denoted as $\triangle x_{l,d}$ ($\triangle x_{l,d} = x_l - x_d$). $\triangle x_{l,d}$ is always zero in the case of FF as the lit lamp position equals the expected aircraft position. The mean value of $\triangle x_{l,d}$ is close to zero in the case of $PI_2$. In contrast, the mean value of $\triangle x_{l,d}$ is much larger in the case of PID, which indicates that the lit lamp position tends to go ahead of the expected aircraft position due to the time delay of pilots' responses to the maneuvering commands. In this way, the conformance errors can be reduced comparing to the cases of FF and $PI_2$.

A typical example of the abovementioned results is presented in Fig. 12. The actual and expected taxiing speeds are presented in Fig. 12(a), which shows in general a good conformance to the expected speed defined by the 4DT using any of the three lamp control strategies. However, the actual taxiing speeds can have noticeable deviation at certain points due to the pilot's delay in responding to the relative speed or distance changes. This helps to explain the cause of the 4DT conformance error as well as the reason for the aircraft tendency of falling behind the expected position in the cases of FF and $PI_2$. As shown in Fig. 12(a), the aircraft starts taxiing with a delay of a few seconds compared to the start time of the assigned 4DT which is set to 0 for clarity. This delay leads to a conformance error of more than 40 m as shown in Fig. 12(b). Similar situation occurs for the long acceleration phase near 400 s where the aircraft fails to start acceleration immediately. Another typical situation of speed deviation occurs when the expected speed changes from an acceleration stage to a constant speed stage, where the actual speeds often overshoot the expected one in the cases of FF and PID. The overshoots of the speed using the PID lamp controller tend to be larger, resulting in larger taxiing speeds than those in the cases of FF and $PI_2$. Larger taxiing speeds often help in reducing the conformance error since aircraft tend to fall behind the expected position, as indicated in Fig. 12(b).

**Table 2**
Comparison of the mean conformance errors and two additional distance metrics.

| Lamp control | Mean conformance error (m) | Mean $\triangle x_{l,a}$ (m) | Mean $\triangle x_{l,d}$ (m) |
|---|---|---|---|
| FF | −48.2 | 48.2 | 0 |
| $PI_2$ | −48.9 | 48.4 | −0.5 |
| PID | −5.6 | 49.0 | 43.4 |

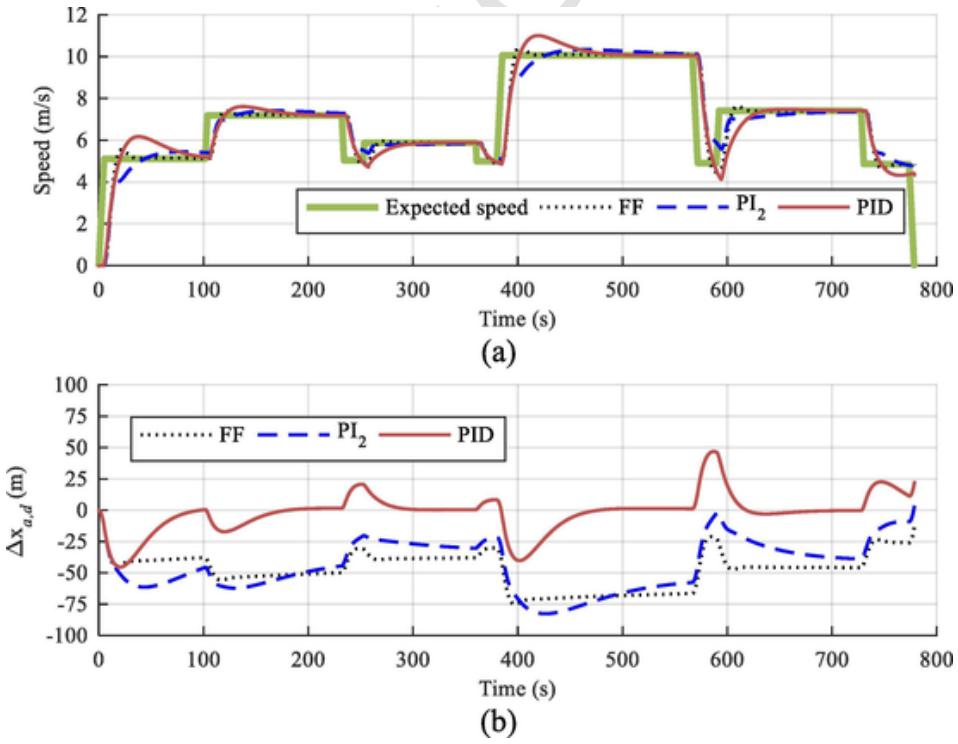


**Fig. 12.** A typical example of the results using different lamp control strategies. (a) Actual and expected taxiing speeds. (b) Conformance errors.

It is worth noting that in the abovementioned test, the values of parameter $K_{p,1}$ $K_{p,1}$and $K_{p,2}$ in the pilot driving model are fixed, set to the average values over 11 pilots identified in the earlier work (Haus et al., 2011; Urvoy, 2014). However, the conformance performance could be influenced when considering the variance of $K_{p,1}$ $K_{p,1}$and $K_{p,2}K_{p,2}$. An illustration is presented in Fig. 13 to demonstrate the impact of $K_{p,1}$ and $K_{p,2}$ on the conformance error. Here the same instance as the one shown in Fig. 12 is used, while $K_{p,1}$ or $K_{p,2}$ changes with a fixed step size from the smallest to the largest values presented in Urvoy (2014). The resulting conformance errors are shown in Fig. 13(a) and Fig. 13(b), respectively. In each figure, the three subfigures from top to bottom corre-

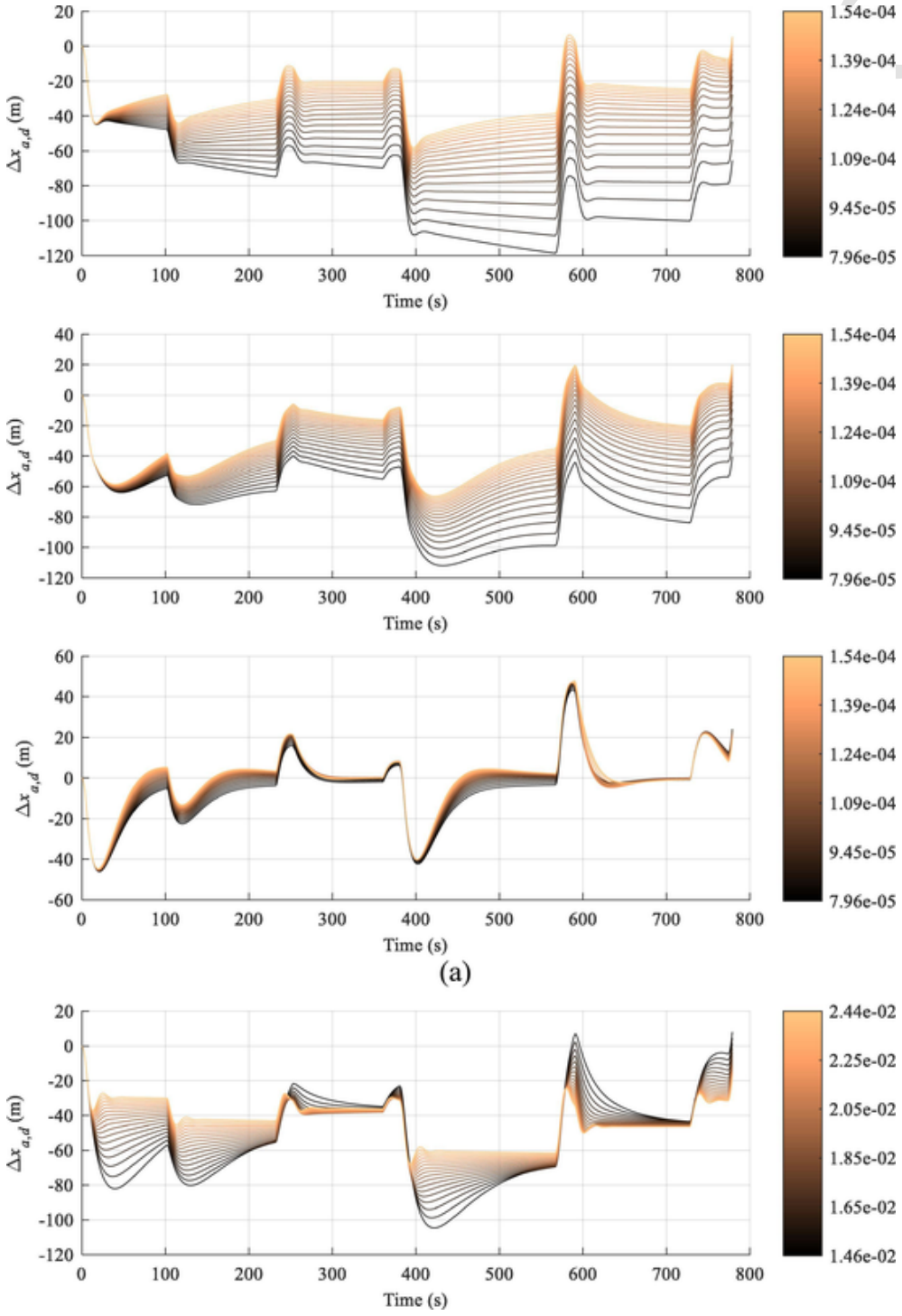


**Fig. 13.** An illustration of the conformance error impacted by varied parameter values. (a) Results for varied $K_{p,1}$. (b) Results for varied $K_{p,2}$.

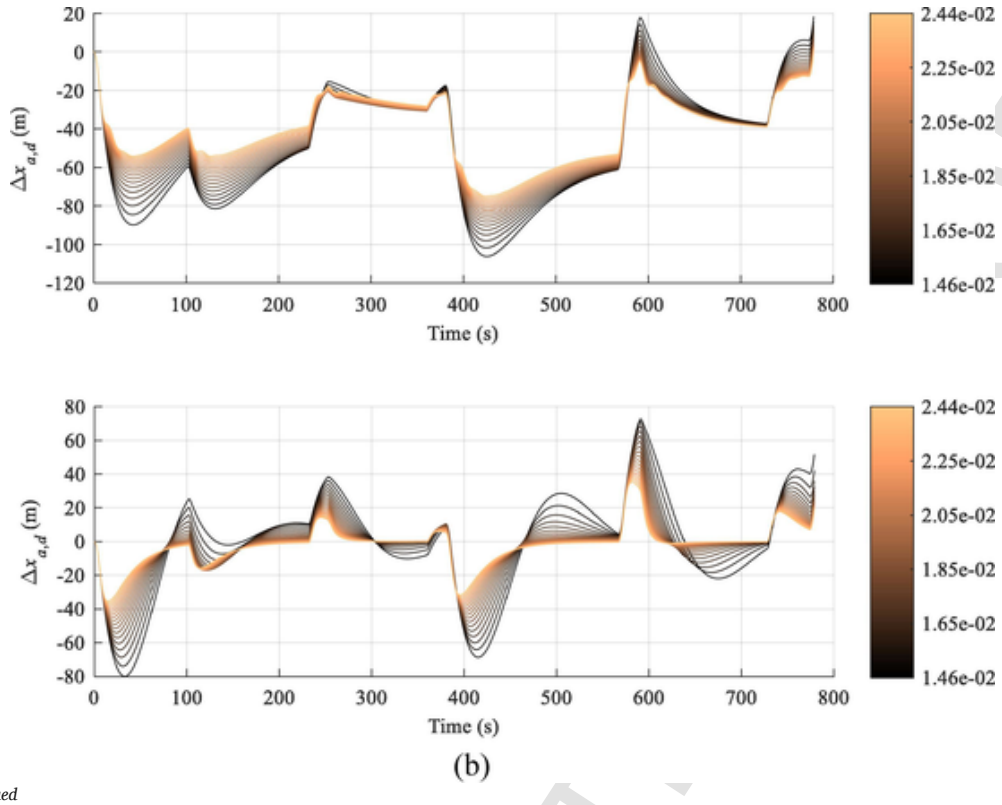


Fig. 13. *Continued*

spond to the FF, $PI_2$ and PID lamp control strategies, respectively. The values of $K_{p,1}$ and $K_{p,2}$ are represented by different colors as shown in the colorbar on the right side of each subfigure. It can be observed that larger values of $K_{p,1}$ $K_{p,1}$and $K_{p,2}$ tend to result in better conformance to the assigned trajectories, which is especially visible in the results of FF and $PI_2$ for varied $K_{p,1}$ as shown in Fig. 13(a).

Furthermore, to investigate the influence of varied $K_{p,1}$ and $K_{p,2}$ on the overall conformance performance, an additional computational test is performed. Specifically, the 18 pairs of valid parameter values identified in Urvoy (2014) are randomly assigned to $K_{p,1}$ and $K_{p,2}$ of each problem instance in the dataset. Other settings including the lamp controller parameters are kept unchanged as described in Section 4.1. For the three investigated lamp control strategies (i.e. FF, $PI_2$ and PID), the resulting mean conformance errors are −54.0, −53.4 and −6.2 m, respectively. Compared with the results in Table 2, it can be seen that the conformance errors have slightly enlarged after considering the variance of $K_{p,1}$ and $K_{p,2}$. However, the impact on the overall conformance is not significant.

### *4.3. Temporal constraint violation*

The existence of the conformance error could make aircraft unable to arrive at the control points at the expected time as specified by the 4DT. The deviation from the expected arrival time can further lead to two or more aircraft occupying the same zone of the taxiway simultaneously, which may violate the distance constraint imposed for the ground movement safety. Large deviation from the expected arrival times may even change the order of aircraft visiting the same zone of the taxiway, leading to deadlocks due to head-on encounter of two aircraft or circular waiting of multiple aircraft (ter Mors and Witteveen, 2009). As mentioned in Section 4.1, when generating the 4DTs, we can impose a minimal time separation $\epsilon$ between consecutive occupancies to tolerate arrival time deviations. However, it is not desired to impose an overly conservative time separation between aircraft as we want to guarantee high ground movement efficiency. A reasonable approach to determine the minimal time separation is to find whether there will be simultaneous occupancies due to arrival time deviations.

According to the assigned 4DT, the time at which an aircraft is expected to enter and exit a zone of the taxiway can be determined. Let $l_s = (a_i, a_{i+1}, \ldots, a_{i+k})$ be the sequence of aircraft occupying taxiway zone $s$, and $t_m^+$ and $t_m^-$ be the time aircraft $a_{i+m}$ $(1 \leqslant m \leqslant k)$ enters and exits $s$, respectively. The expected time separation between aircraft $a_{i+m}$ and $a_{i+m-1}$ is $t_m^+ - t_{m-1}^-$. If a minimal time separation $\epsilon$ between consecutive occupancies is imposed for the assigned 4DTs, we have $t_m^+ - t_{m-1}^- \geqslant \epsilon$. The actual time separations can be smaller than $\epsilon$ due to the 4DT conformance errors. When the actual time separation is less than zero, the temporal constraint will be violated and a simultaneous occupancy appears. In this case, subsequent aircraft will enter the corresponding zone of the taxiway before it is cleared (i.e. before the previous aircraft leaves).

In this section, the relationship between the occurrence of temporal constraint violations and the value of the minimal time separation $\epsilon$ is investigated using the PID lamp controller, as it has the best overall performance among the three lamp control strategies. The empirical cumulative distributions of the actual time separations between consecutive occupancies over all the zones of the taxiway are presented in Fig. 14, which correspond to $\epsilon = 0$, $\epsilon = 5$ and $\epsilon = 10$ seconds, respectively. For clarity, only time separations smaller than 20 s are included in Fig. 14. The results indicate that fewer temporal constraint violations occur when larger minimal time separations are kept between the assigned 4DTs. However, the temporal constraint violations cannot be fully eliminated due to the instances which still have overly large conformance errors.

Table 3 compares the number of temporal constraint violations with the result estimated for the situation when the conformance error can be reduced by half. This is obtained by scaling the original conformance error $\triangle x_{a,d}$ by a factor of 0.5. Let $\alpha$ be the scaling factor, then the scaled conformance error is $\triangle \hat{x}_{a,d} = \alpha \triangle x_{a,d}$, and the corresponding actual aircraft position is $\hat{x}_a = x_d + \triangle \hat{x}_{a,d}$. The actual time separations can be determined according to $\hat{x}_a$. The results demonstrate that if the conformance error could be reduced by half, no temporal constraint violations would occur when the minimal time separation is set to 10 s. Moreover, it can be observed that the majority of temporal constraint violations can already be eliminated in this case with the minimal time separation being 5 s only.

In view of the fact that the conformance error is usually inevitable and any attempt to reduce this error will have cost implications, analysing its impact on the temporal constraint violation can provide useful insight in setting appropriate bounds of the conformance error. These bounds could be set up based on a given control point arrival time deviation tolerance, and can be further used as a guideline to design suitable lamp controllers.

### *4.4. Estimation of fuel consumption*

The assigned 4DTs have been optimised to represent the most cost effective way for aircraft taxiing on ground; any deviations from the assigned 4DTs will lead to increased airport opportunity costs, aircraft maintenance costs or fuel costs (Chen et al., 2016b). In this section, we focus on investigating the impact of such deviations on the fuel consumption. The calculation of the fuel burnt during taxiing is based on the parameters presented in Table 1. The fuel consumption of an aircraft taxiing according to an assigned 4DT is determined as follows:

$$M_{fuel} = \int_0^T f \cdot dt \tag{3}$$

where $f$ and $T$ are respectively the fuel flow rate and taxiing time. Similar to Chen et al. (2016b) and Nikoleris et al. (2011), the fuel flow rates for different engine thrust levels are determined by interpolation or extrapolation according to the known fuel flow rates at 7% and 30% of the rated engine thrust (see Table 1). These two fuel flow rates respectively correspond to the idle and ap-

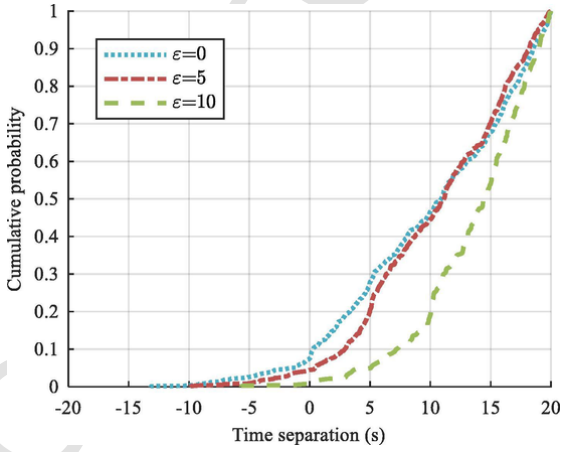


**Fig. 14.** Empirical cumulative distribution of the time separations.

**Table 3**
Number of temporal constraint violations.

| | PID controller | Reduced conformance error |
|---|---|---|
| $\epsilon = 0$ | 53 | 40 |
| $\epsilon = 5$ | 25 | 5 |
| $\epsilon = 10$ | 4 | 0 |

proach conditions of the aircraft engine, as described in the ICAO Aircraft Engine Emissions Databank (EASA, 2018). The engine thrust level is the ratio of the thrust force $F_T$ to the rated engine thrust, where $F_T$ is determined according to (1).

According to the assigned 4DTs, the mean fuel consumption per aircraft assuming perfect conformance is 79.0 kg. The estimated fuel consumption with different levels of conformance errors are presented in Table 4, together with the increase rates compared to the fuel consumption assuming perfect conformance. The levels of conformance errors are represented by different values of the scaling factor $\alpha$ introduced in Section 4.3. The results show an obvious impact of the conformance error on the estimated fuel consumption, where a fuel consumption decrease of no less than 0.5% occurs for every 25% reduction of the conformance error within the investigated range.

## 5. Conclusion

This paper presents a comprehensive investigation of 4DT based FtG guidance for trajectory-based taxiing operations. The taxiing system with FtG guidance is simulated by integrating the first-order control theoretic model of aircraft taxiing dynamics, the pilot driving model and the ground navigation lamp controller. The 4DT conformance errors using three different lamp control strategies (including a newly proposed PID lamp controller) are compared to demonstrate the importance of having an appropriate lamp control method for effective FtG guidance. Based on the proposed PID lamp controller which has the best performance among the investigated lamp control strategies, the temporal constraint violation and fuel consumption increase due to the conformance errors are analysed. The results demonstrate the feasibility of FtG as an augmented guidance means to provide the 4DT information given that a suitable lamp control approach can be developed.

However, the conformance errors are inevitable, causing aircraft unable to reach the control points on time. This requires to impose sufficient buffer between aircraft when generating the 4DTs to avoid temporal constraint violations. Adding a universal minimal time separation at all zones of the taxiway may not be an optimal approach concerning both the robustness and efficiency of the ground movements. A more effective approach would be adding variable time separations according to the distribution of conformance errors in different zones of the taxiway. This requires an integrated optimisation of 4DT generation and taxiing guidance based on an effective prediction of the conformance errors, which is worth investigation in future work.

In addition to constraint violations, conformance errors would also lead to increased fuel consumption. As demonstrated in the presented study, when a fuel-efficient 4DT is assigned to the aircraft, the larger the conformance errors are, the more fuel will usually be consumed during taxiing. Improved lamp control strategies can reduce the conformance error. However, even for the PID controller that has the smallest mean conformance error among the investigated lamp control strategies, there is still 4.8% increase of the fuel consumption. This indicates the need to develop more sophisticated navigation lamp controllers in future.

## CRediT authorship contribution statement

**Tianci Zhang:** Conceptualization, Methodology, Software, Validation, Writing - original draft, Funding acquisition. **Michal Weiszer:** Methodology, Software, Writing - review & editing. **Jun Chen:** Conceptualization, Methodology, Writing - review & editing, Supervision, Funding acquisition.

## Acknowledgement

This work is supported in part by the Engineering and Physical Sciences Research Council (EPSRC) under Grant EP/N029496/1 and EP/N029496/2, the Joint Research Funds of National Natural Science Foundation of China and Civil Aviation Administration of China under Grant U1633105 and U1933202, and the Natural Science Foundation of Jiangsu Higher Education Institutions of China under Grant 19KJB580013. The authors would like to thank the anonymous reviewers for their detailed and constructive comments.

## Appendix A. Supplementary material

Supplementary data to this article can be found online at https://doi.org/10.1016/j.trc.2020.102632.

**Table 4**
Fuel consumption estimations.

| | PID controller | $\alpha = 0.75$ | $\alpha = 0.5$ | $\alpha = 0.25$ |
|---|---|---|---|---|
| Mean fuel consumption (kg) | 82.8 | 82.2 | 81.7 | 81.3 |
| Increase rate (%) | 4.8 | 3.9 | 3.4 | 2.8 |

## References


ADB SAFEGATE. AGLAS - system to control and monitor individual airfield lights. https://adbsafegate.com/documents/2773/en/data-sheet-aglas (Jan. 20, 2020 accessed)

Ahmed, K.I., 1999. Modeling drivers' acceleration and lane changing behavior. (PhD), Massachusetts Institute of Technology.

Åström, K.J., Hägglund, T., 2006. Advanced PID control. Research Triangle Park, NC: ISA-The Instrumentation, Systems, and Automation Society.

Brownlee, A E I, Weiszer, M, Chen, J, Ravizza, S, Woodward, J R, Burke, E K, 2018. A fuzzy approach to addressing uncertainty in airport ground movement optimisation. Transportation Res. Part C: Emerging Technol. 92, 150–175. doi:10.1016/j.trc.2018.04.020.

Carotenuto, S., 2005. State of the art in A-SMGCS. https://core.ac.uk/download/pdf/11103904.pdf (Jan. 19, 2020 accessed).

Chen, J, Weiszer, M, Locatelli, G, Ravizza, S, Atkin, J, Stewart, P, Burke, E, 2016. Toward a more realistic, cost effective and greener ground movement through active routing: a multi-objective shortest path approach. IEEE Trans. Intell. Transp. Syst. 17 (12), 3524–3540. doi:10.1109/TITS.2016.2587619.

Chen, J, Weiszer, M, Stewart, P, Shabani, M, 2016. Toward a more realistic, cost effective and greener ground movement through active routing: part 1-optimal speed profile generation. IEEE Trans. Intell. Transp. Syst. 17 (5), 1196–1209. doi:10.1109/TITS.2015.2477350.

Eurocontrol, 2010. Definition of A-SMGCS implementation levels. https://www.eurocontrol.int/sites/default/files/field_tabs/content/documents/nm/airports/a-smgcs-definition-of-implemetation-levels-v1-2-20100630.pdf (Feb. 25, 2017 accessed).

Eurocontrol, 2017. Airport CDM implementation manual version 5. https://www.eurocontrol.int/archive_download/all/node/10373 (Jul. 19, 2018 accessed).

European Aviation Safety Agency (EASA). ICAO Aircraft Engine Emissions Databank. https://www.easa.europa.eu/easa-and-you/environment/icao-aircraft-engine-emissions-databank (Jul. 25, 2018 accessed).

European Commission, 2017. Follow-the-greens: the future of guidance is green. https://ec.europa.eu/transport/modes/air/ses/ses-award/projects/2017-follow-greens-future-guidance-green_it (Jul. 19, 2018 accessed).

Haus, S, Sendobry, A, Urvoy, C, Klingauf, U, 2011. Control theoretic concept for intuitive guidance of pilots during taxiing. In: Paper Presented at the IEEE/AIAA 30th Digital Avionics Systems Conference (DASC). doi:10.1109/DASC.2011.6096097.

Hodel, A S, Hall, C E, 2001. Variable-structure PID control to prevent integrator windup. IEEE Trans. Ind. Electron. 48 (2), 442–451. doi:10.1109/41.915424.

Hooey, B.L., Cheng, V.H., Foyle, D.C., 2014. A concept of operations for far-term surface trajectory-based operations (STBO). https://human-factors.arc.nasa.gov/publications/STBO%20ConOps_TM_2014_218354.pdf (Jul. 19, 2018 accessed).

ICAO, 2004. Advanced surface movement guidance and control systems (A-SMGCS) manual. http://www.icao.int/Meetings/anconf12/Document%20Archive/9830_cons_en%5B1%5D.pdf (Mar. 20, 2018 accessed).

Katz, E.S., 2000. Evaluation of a prototype advanced taxiway guidance system (ATGS). https://ntlrepository.blob.core.windows.net/lib/16000/16400/16401/PB2000103678.pdf (Jan. 20, 2020 accessed).

Martin, P., Hudgell, A., Vial, S., Bouge, N., 1998. FASTER: Future ATFM-AO-Airport synergies towards enhanced operations. https://www.eurocontrol.int/archive_download/all/node/10082 (Jan. 20, 2020 accessed).

Nikoleris, T, Gupta, G, Kistler, M, 2011. Detailed estimation of fuel consumption and emissions during aircraft taxi operations at Dallas/Fort Worth International Airport. Transportation Res. Part D: Transport Environ. 16 (4), 302–308. doi:10.1016/j.trd.2011.01.007.

Okuniek, J N, Gerdes, I, Jakobi, J, Ludwig, T, Hooey, B L, Foyle, D, Zhu, Z, 2016. A concept of operations for trajectory-based taxi operations. In: Paper Presented at the 16th AIAA Aviation Technology, Integration, and Operations Conference. doi:10.2514/1.I010699.

Ravizza, S, Atkin, J A, Burke, E K, 2014. A more realistic approach for airport ground movement optimisation with stand holding. J. Sched. 17 (5), 507–520. doi:10.1007/s10951-013-0323-3.

Ravizza, S, Chen, J, Atkin, J A D, Stewart, P, Burke, E K, 2014. Aircraft taxi time prediction: comparisons and insights. Appl. Soft Comput., 14, Part C 397–406. doi:10.1016/j.asoc.2013.10.004.

Schuster, W, Ochieng, W, 2014. Performance requirements of future trajectory prediction and conflict detection and resolution tools within SESAR and NextGen: framework for the derivation and discussion. J. Air Transport Manage. 35, 92–101. doi:10.1016/j.jairtraman.2013.11.005.

Straube, K, Roßbach, M, Vieten, B D, Hahn, K, 2017. Follow-the-greens: the controllers' point of view results from a SESAR real time simulation with controllers. In: Advances in Human Aspects of Transportation. Springer, pp. 837–849.

Tang, X, An, H, Wang, C, 2012. Conflict-avoidance-oriented airport surface-taxiing guidance lights system model. J. Guidance, Control, Dyn. 35 (2), 674–681. doi:10.2514/1.54693.

ter Mors, A, Witteveen, C, 2009. Plan repair in conflict-free routing. In: Next-Generation Applied Intelligence. Springer, pp. 46–55.

Urvoy, C., 2014. Conceptual design and evaluation of a 4D taxi guidance system for transport aircraft. (PhD), TU Darmstadt. (in German).

Urvoy, C, Oehme, A, Drege, C, Sendobry, A, Klingauf, U, 2010. Conceptual validation of advanced pilot guidance-systems - a field test report. IFAC Proc. Volumes 43 (13), 356–361. doi:10.3182/20100831-4-FR-2021.00063.

Weiszer, M, Chen, J, Locatelli, G, 2015. An integrated optimisation approach to airport ground operations to foster sustainability in the aviation sector. Appl. Energy 157, 567–582. doi:10.1016/j.apenergy.2015.04.039.

Weiszer, M, Chen, J, Stewart, P, 2015. A real-time active routing approach via a database for airport surface movement. Transportation Res. Part C: Emerging Technol. 58, 127–145. doi:10.1016/j.trc.2015.07.011.

Zhang, T, Ding, M, Zuo, H, 2018. Improved approach for time-based taxi trajectory planning towards conflict-free, efficient and fluent airport ground movement. IET Intel. Transport Syst. 12 (10), 1360–1368. doi:10.1049/iet-its.2018.5193.

Zhang, T, Ding, M, Zuo, H, Chen, J, Weiszer, M, Qian, X, Burke, E K, 2018. An online speed profile generation approach for efficient airport ground movement. Transportation Res. Part C: Emerging Technol. 93, 256–272. doi:10.1016/j.trc.2018.05.030.

Zhou, D, Gao, X, Liu, G, Mei, C, Jiang, D, Liu, Y, 2011. Randomization in particle swarm optimization for global search ability. Expert Syst. Appl. 38 (12), 15356–15364. doi:10.1016/j.eswa.2011.06.029.